PROCEEDINGS OF SCIENCE

Radiative and Rare Semileptonic B Decays

Mikołaj Misiak*
University of Warsaw and Karlsruhe Institute of Technology
E-mail: `Mikolaj.Misiak@fuw.edu.pl`

Loop-generated rare B-meson decays provide important constraints on new physics irrespectively of whether their measured properties agree or not with the Standard Model predictions. For generic theories beyond Minimal Flavour Violation, the number of interesting observables is quite large. Several recent advances in the field are discussed in this talk.

Flavor Physics and CP Violation 2010
May 25-29,2010
Turin, Italy

*Speaker.

PoS(FPCP 2010)025

1. Introduction

Radiative and rare semileptonic B-meson decays have been extensively studied at the B factories, LEP and the TeVatron. New results from the LHCb are expected soon. The number of interesting observables is quite large. The prominent one is $\mathscr{B}(\bar{B} \to X_{s,d}\gamma)$ with a certain lower cut E_0 on the photon energy. It provides the simplest way to constrain the SM-like loop-generated $bs\gamma$ coupling. Moments of the photon spectrum in this inclusive decay can be tested against predictions based on non-perturbative HQET parameters determined from the semileptonic $\bar{B} \to X_c l \bar{\nu}$ spectra. Isospin asymmetries are very small in the SM, and unlikely to be modified by new physics. However, their precise measurement would remove one of the most important non-perturbative uncertainties in the SM prediction for the total rate. Mixing-induced CP-asymmetries are also very small in the SM due to the left-handed photon dominance in the decay amplitude. Their measurement puts bounds on possible opposite-chirality operators in the effective Lagrangian. Finally, the d/s ratio (i.e. $\mathscr{B}(\bar{B} \to X_d\gamma)/\mathscr{B}(\bar{B} \to X_d\gamma)$) provides interesting information on V_{td}/V_{ts}.

For the closely related inclusive $\bar{B} \to X_{s,d} l^+ l^-$ decay, we may consider the same observables as for $\bar{B} \to X_{s,d}\gamma$, just replacing the photon energy by the lepton pair one. However, more options are available thanks to the four-body kinematics. In particular, studying various observables as functions of the dilepton invariant mass squared $q^2 = m^2_{l^+l^-}$, we can extract relative contributions from several effective operators. The forward-backward (FB) asymmetry is even more efficient in this respect. Apart from the total rate and the FB-asymmetry (as functions of q^2), another inclusive observable could provide independent information. Using three alternative observables called H_T, H_A and H_L has been advocated in Ref. [1].

In the exclusive $B \to V\gamma$ case ($V = K^\star, \rho, \omega$), the decay widths are quite uncertain on the theory side. However, many uncertainties cancel in the isospin and CP asymmetries, as well as in the d/s ratios. In the latter case, $\mathscr{B}(B \to \rho^0\gamma)/\mathscr{B}(B \to K^\star\gamma)$ is most useful from the theory standpoint. Its current effect on the overall CKM fit is miniscule due to large experimental errors, but nevertheless it gives us a non-trivial consistency check.

From the LHCb perspective, the most interesting channels are the exclusive $B \to K l^+ l^-$ and $B \to K^\star l^+ l^-$ modes. In the latter case, when $K^{0\star}$ decays to $K^+\pi^-$, high-statistics angular analysis is possible despite the small overall branching ratio ($\sim 10^{-6}$). Properly chosen integrated observables can be used to efficiently constrain potential new physics effects.

The current status and future perspectives of the radiative and rare semileptonic B decays have been thoroughly reviewed in a very recent paper by T. Hurth and M. Nakao [2]. In this talk, I will concentrate on just a couple of observables.

2. The effective theory

A convenient framework to analyze processes which take place at scales $\mu \sim m_b$ or lower is an effective theory that arises after decoupling of W, Z, t, H^0 and all the Beyond-Standard-Model (BSM) particles with masses $m_i \gg m_b$. Assuming that all the relevant BSM particles can be decoupled, we obtain an effective Lagrangian of the form

$$\mathscr{L}_{\rm eff} = \mathscr{L}_{\rm QCD\times QED}(u,d,s,c,b;e,\mu,\tau) \; + \; \frac{4G_F}{\sqrt{2}} \sum_i f^i_{\rm CKM} C_i Q_i \; + \; (\dim \geq 6 \text{ operators}). \tag{2.1}$$

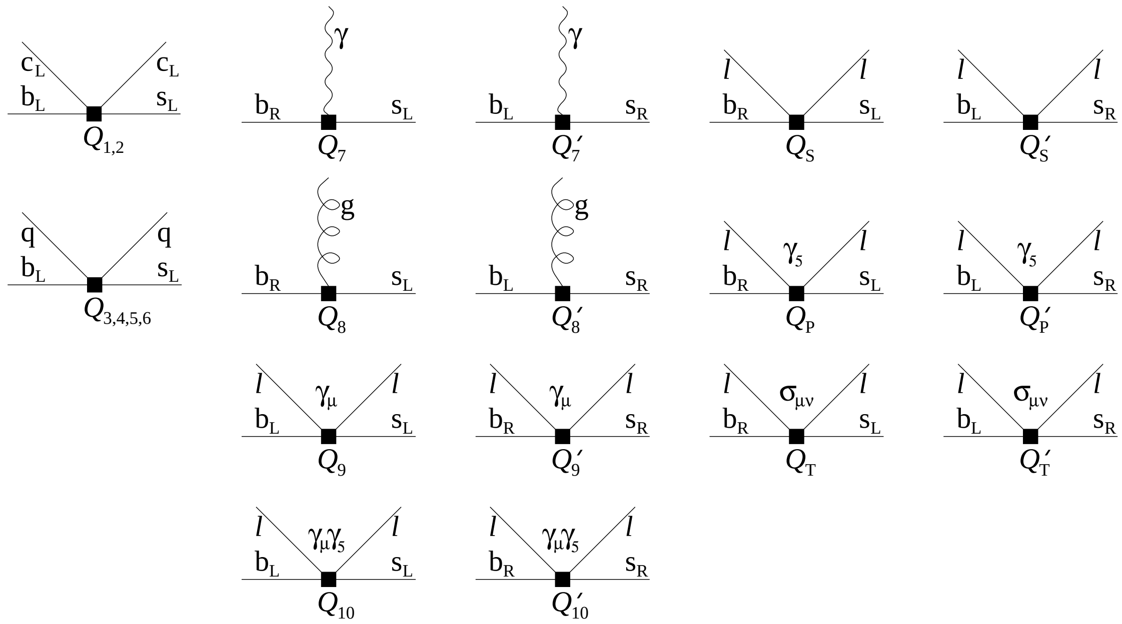

Figure 1: Operator vertices that are relevant for $b \to s\gamma$ and $b \to sl^+l^-$. In addition to them, double-gluon vertices of Q_8 and Q_8' enter beyond the leading order in QCD.

Here, Q_i are operators of dimension 5 or 6, while C_i are their Wilson coefficients. In the SM or any weakly-coupled BSM theory, C_i are perturbatively calculable functions of masses, couplings and renormalization scales.

Fig. 1 contains a collection of operator vertices that are relevant for $b \to s\gamma$ and $b \to sl^+l^-$, under the assumption that no relevant BSM effects occur in the four-quark sector. In the SM, only the operators Q_1–Q_{10} from the first two columns matter. These statements hold up to $\mathcal{O}\left(m_s^2/m_b^2, \alpha_{\rm em}\right)$ corrections.

3. Exclusive $\bar{B}^0 \to \bar{K}^{0\star} l^+ l^-$.

The exclusive decay $\bar{B}^0 \to \bar{K}^{0\star} l^+ l^-$ followed by $\bar{K}^{0\star} \to K^- \pi^+$ is particularly interesting because many independent constraints on the Wilson coefficients can be extracted from the full angular distribution of this decay chain. The differential decay width is conveniently written as follows:

$$\frac{d^4\Gamma}{dq^2\, d\cos\theta_l\, d\cos\theta_K\, d\phi} = \frac{9}{32\pi} J(q^2, \theta_l, \theta_K, \phi), \tag{3.1}$$

where

$$\begin{aligned} J(q^2, \theta_l, \theta_K, \phi) \;=\;& J_{1s} \sin^2\theta_K + J_{1c} \cos^2\theta_K + \left(J_{2s} \sin^2\theta_K + J_{2c} \cos^2\theta_K\right) \cos 2\theta_l \\ &+ J_3 \sin^2\theta_K \sin^2\theta_l \cos 2\phi + J_4 \sin 2\theta_K \sin 2\theta_l \cos\phi + J_5 \sin 2\theta_K \sin\theta_l \cos\phi \\ &+ \left(J_{6s} \sin^2\theta_K + J_{6c} \cos^2\theta_K\right) \cos\theta_l + J_7 \sin 2\theta_K \sin\theta_l \sin\phi \\ &+ J_8 \sin 2\theta_K \sin 2\theta_l \sin\phi + J_9 \sin^2\theta_K \sin^2\theta_l \sin 2\phi. \end{aligned} \tag{3.2}$$

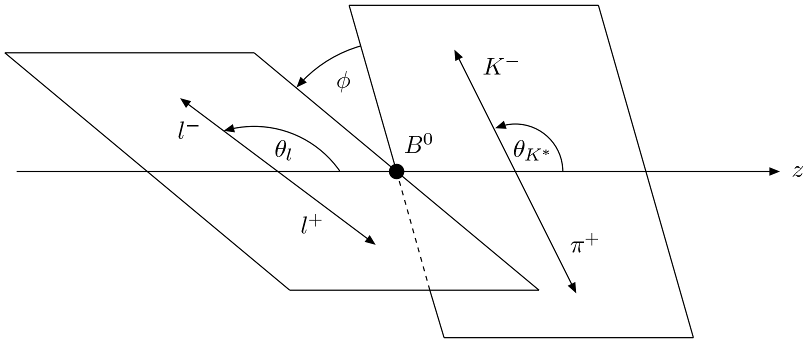

Figure 2: Angle definitions in the $\bar{B}^0 \to \bar{K}^{0\star} l^+ l^-$ differential spectrum.

Here, q^2 is the dilepton invariant mass squared, while the meaning of the angles is explained in Fig. 2. The important conventions to remember are that θ_l is measured in the dilepton c.m.s., θ_K — in the $K^-\pi^+$ c.m.s., and ϕ — in the $\bar{B}^0$ rest frame. The formula in Eq. (3.2) corresponds to a narrow peak approximation for $\bar{K}^{0*}$.

The quantity $J(q^2)$ in Eq. (3.2) can be expressed in terms of complex spin amplitudes $A_\perp^{L,R}$, $A_\parallel^{L,R}$, $A_0^{L,R}$, $(A_t,\, A_S,\, \ldots)$ that depend linearly on the Wilson coefficients and q^2-dependent form-factors. In the large E_{K^*} limit $(m_{K^*}/E_{K^*} \sim \Lambda/m_b \ll 1)$ only two form-factors $\xi_\perp(q^2)$ and $\xi_\parallel(q^2)$ remain, up to $\mathcal{O}(\alpha_s, \Lambda/m_b)$ effects (see e.g. Ref. [3]). Taking this fact into account, it is possible to derive constraints on the Wilson coefficients by considering ratios of the spin amplitudes in which the form-factors ξ cancel out. Next, one can fit those ratios to data using various weighted integrals of the measured angular distribution. There are obviously very many options for applying this algorithm in practice, and a whole industry devoted to such analyses has developed in the past few years.

The most recent step forward has been made in Ref. [4]. Four (real) relations between the spin amplitudes have been identified. Next, ratios like

$$A_T^{(2)} = \frac{|A_\perp^L|^2 + |A_\perp^L|^2 - |A_\parallel^L|^2 - |A_\parallel^R|^2}{|A_\perp^L|^2 + |A_\perp^L|^2 + |A_\parallel^L|^2 + |A_\parallel^R|^2} = \frac{2\left[\mathrm{Re}\,(C_{10}' C_{10}^*) + F^2 \mathrm{Re}\,(C_7' C_7^*) + F \mathrm{Re}\,(C_7' C_9^*)\right]}{|C_{10}|^2 + |C_{10}'|^2 + F^2\left(|C_7|^2 + |C_7'|^2\right) + |C_9|^2 + 2F\,\mathrm{Re}\left(C_7 C_9^*\right)},$$

$$A_T^{(5)} = \frac{|A_\perp^L A_\parallel^{R*} + A_\perp^{R*} A_\parallel^L|}{|A_\perp^L|^2 + |A_\perp^L|^2 + |A_\parallel^L|^2 + |A_\parallel^R|^2} \stackrel{\mathrm{SM}}{=} \frac{1}{2}\,\frac{(FC_7 + C_9)^2 - C_{10}^2}{(FC_7 + C_9)^2 + C_{10}^2} \tag{3.3}$$

were considered including $\mathcal{O}(\Lambda/m_b)$ uncertainties in their numerical values. Here, $F = 2m_b m_B/q^2$, while C_7 and $C_9(q^2)$ stand for the so-called "effective" coefficients [5]. A sample effect of the BSM-modified Wilson coefficients on $A_T^{(5)}$ is shown in Fig. 3. Its dependence on q^2 in the SM (for $C_9 \sim -C_{10} \sim 4$) is compared to a situation where either C_{10}' or $\Delta C_9^{\mathrm{NP}} \equiv C_9^{\mathrm{BSM}} - C_9^{\mathrm{SM}}$ is set to $2e^{i\pi/8}$. It is evident that an accurate enough determination of $A_T^{(5)}$ is going to provide important constraints on models where new contributions to the Wilson coefficients are of the same order as the SM ones. However, if the BSM effects give only small corrections to the SM values, and no new operators arise (like in the MSSM with Minimal Flavour Violation (MFV)), then the $\mathcal{O}(\Lambda/m_b)$ uncertainties will most probably make such effects unobservable in the considered exclusive decay.

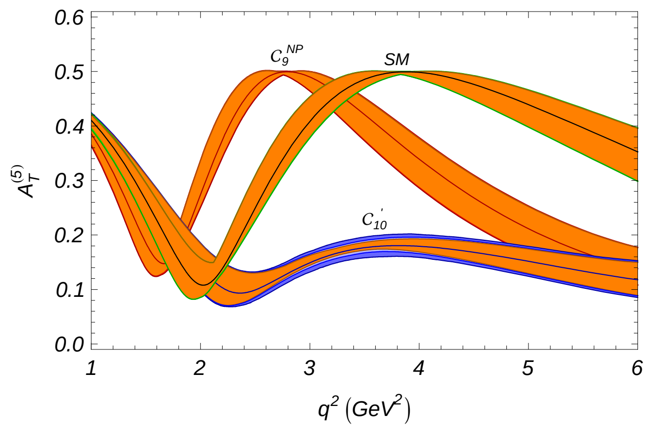

Figure 3: The ratio $A_T^{(5)}$ for either C'_{10} or $\Delta C_9^{\rm NP}$ set to $2e^{i\pi/8}$ (Fig. 16 from Ref. [4]).

4. Combined constraints on the Wilson coefficients

Apart from considering future prospects for particular decay modes, it is interesting to verify what constraints on the Wilson coefficients can be derived by combining several well-determined observables in the radiative and rare semileptonic B decays. Such a question has recently been analyzed in Ref. [6]. Six observables were taken into account, namely $\mathscr{B}(\bar{B} \to X_s \gamma)$, $S(B \to K^* \gamma)$, $\mathscr{B}(\bar{B} \to X_s l^+ l^-)_{1-6\,{\rm GeV}^2}$, $F_{\rm L}(\bar{B}^0 \to \bar{K}^* \mu^+ \mu^-)_{1-6\,{\rm GeV}^2}$, $A_{\rm FB}(\bar{B}^0 \to \bar{K}^* \mu^+ \mu^-)_{1-6\,{\rm GeV}^2}$ and $S_5(\bar{B}^0 \to \bar{K}^* \mu^+ \mu^-)_{1-6\,{\rm GeV}^2}$. The CP-averaged forward-backward asymmetry $A_{\rm FB}$ and the asymmetry called S_5 are proportional to the following angular integrals:

$$A_{FB}(q^2) \sim \left(\frac{d(\Gamma + \bar{\Gamma})}{dq^2} \right)^{-1} \left[\int_0^1 - \int_{-1}^0 \right] d\cos\theta_l \, \frac{d^2(\Gamma + \bar{\Gamma})}{dq^2 \, d\cos\theta_l},$$
$$S_5(q^2) \sim \left(\frac{d(\Gamma + \bar{\Gamma})}{dq^2} \right)^{-1} \left[\int_0^{\pi/2} - \int_{\pi/2}^{3\pi/2} + \int_{3\pi/2}^{2\pi} \right] d\phi \, \left[\int_0^1 - \int_{-1}^0 \right] d\cos\theta_l \, \frac{d^2(\Gamma + \bar{\Gamma})}{dq^2 \, d\cos\theta_l \, d\phi}. \tag{4.1}$$

Sample scatter plots from Ref. [6] describing constraints on $C_7^{\rm NP}$, C'_7, $C_9^{\rm NP}$ and C'_{10} are shown in Fig. 4 ($C_i^{\rm NP} \equiv C_i - C_i^{\rm SM}$). In the first row, current measurements have been used for all the considered observables (except S_5, for which no data are available yet). The second row shows a projection for LHCb after analyzing 2fb^{-1} of integrated luminosity, and with inclusion of S_5. A semi-random walk algorithm has been used to test 2.5×10^5 sets of the Wilson coefficient values. The SM central values have been assumed for them in the LHCb projection case. The red points are allowed at 68% C.L., while the remaining ones are shown in blue. Three examples corresponding to particular models with specific parameters are shown by the black dot, green square and blue triangle. These are respectively the SM, the MFV MSSM with extra CP-violating phases, and a certain non-MFV MSSM. Obviously, the SM black dot is at the origin $(0,0)$ in all the plots, and it sometimes gets covered by the green square. It is consistent with all the studied observables, giving $\chi^2/n_{\rm D.O.F} = 0.35$. The two non-BSM scenarios are marginally allowed by the current data, and definitely excluded in the LHCb projection case. The power of rare decay observables and interesting prospects for the future are thus convincingly illustrated.

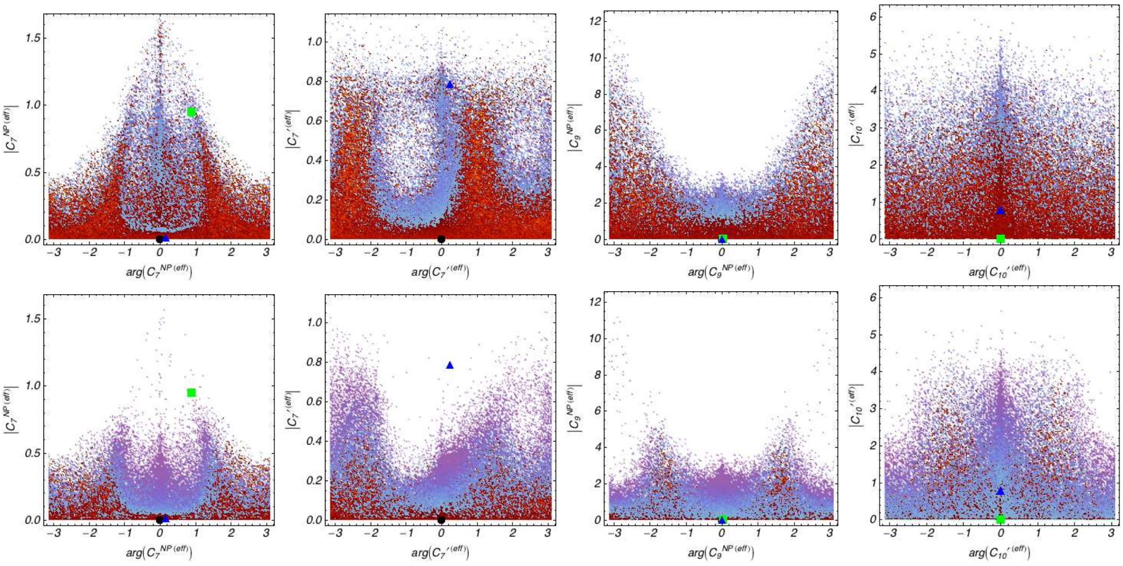

Figure 4: Constraints on the Wilson coefficients $C_7^{\rm NP}$, C_7', $C_9^{\rm NP}$ and C_{10}' from Ref. [6]. In the first row, the currently available data have been used. The second row shows a projection for LHCb after analyzing $2\,{\rm fb}^{-1}$ of integrated luminosity (see the text).

5. Inclusive $\bar{B} \to X_s \gamma$

The current experimental world averages for the $\bar{B} \to X_s \gamma$ branching ratio with $E_\gamma > 1.6\,$GeV in the decaying meson rest frame read:

$$\mathscr{B}(\bar{B} \to X_s \gamma) = \begin{cases} \left(3.55 \pm 0.24_{\rm exp} \pm 0.09_{\rm model}\right) \times 10^{-4} & [7], \\ \left(3.50 \pm 0.14_{\rm exp} \pm 0.10_{\rm model}\right) \times 10^{-4} & [8]. \end{cases} \tag{5.1}$$

They have been obtained by combining the measurements of CLEO [9], BABAR [10] and BELLE [11] with different lower cuts E_0 on the photon energy, ranging from 1.7 to 2.0 GeV. An extrapolation in E_0 down to 1.6 GeV has been performed simultaneously.

Calculations including $\mathscr{O}(\alpha_s^2)$ and $\mathscr{O}(\alpha_{\rm em})$ effects in the SM give [12, 13]

$$\mathscr{B}(\bar{B} \to X_s \gamma) = (3.15 \pm 0.23) \times 10^{-4}, \tag{5.2}$$

where the error is found by adding in quadrature the non-perturbative (5%), perturbative (3% + 3%) and parametric (3%) uncertainties. The result in Eq. (5.2) is consistent with the averages (5.1) at the 1.2σ level. Its evaluation is based on an approximate equality of the hadronic and perturbatively calculable partonic decay widths

$$\Gamma(\bar{B} \to X_s \gamma)_{E_\gamma > E_0} \;\simeq\; \Gamma(b \to X_s^p \gamma)_{E_\gamma > E_0}, \tag{5.3}$$

where X_s^p stands for s, sg, sgg, $sq\bar{q}$, etc. This approximation works well only in a certain range of E_0, namely when E_0 is large ($E_0 \sim m_b/2$) but not too close to the endpoint ($m_b - 2E_0 \gg \Lambda_{\rm QCD}$). Corrections to Eq. (5.3) of various origin have been widely discussed in the literature, most recently in Ref. [14].

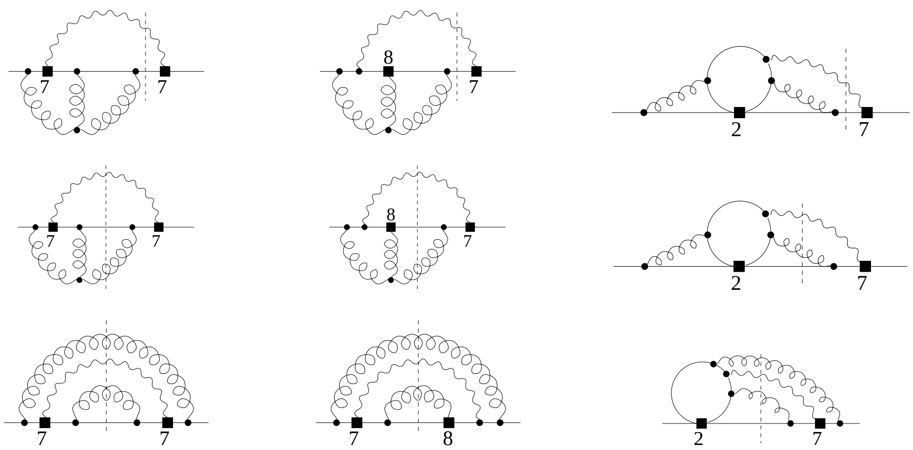

Figure 5: Examples of Feynman diagrams that contribute to G_{77}, G_{78} and G_{27} at $\mathcal{O}(\alpha_s^2)$. Dashed vertical lines mark the unitarity cuts.

The relevant Wilson coefficients at the scale $\mu_b \sim m_b/2$ are presently known up to the Next-to-Next-to-Leading Order (NNLO) in QCD, i.e. up to $\mathcal{O}\left(\alpha_s^2\left(\alpha_s \ln \frac{M_W}{m_b}\right)^n\right)_{n=0,1,2,3,\ldots}$. The necessary matching [15] and anomalous dimension [16] calculations involved Feynman diagrams up to three and four loops, respectively. The partonic decay rate is evaluated according to the formula

$$\Gamma(b \to X_s^p \gamma)_{E_\gamma > E_0} = N \sum_{i,j=1}^{8} C_i(\mu_b) C_j(\mu_b) G_{ij}(E_0, \mu_b), \tag{5.4}$$

where $N = |V_{ts}^\star V_{tb}|^2 \, (G_F^2 m_b^5 \alpha_{\rm em})/(32\pi^4)$. At the NNLO, it is sufficient to restrict our attention to $i, j \in \{1,2,7,8\}$ because the penguin operators have very small Wilson coefficients ($|C_{3,5,6}(\mu_b)| < |C_4(\mu_b)| \sim \ \alpha_s(\mu_b)/\pi$). In the following, we shall treat the two similar operators Q_1 and Q_2 as a single one (represented by Q_2), and consider six independent cases of G_{ij} at the NNLO.

Three of those six cases (G_{77}, G_{78} and G_{27}) involve the photonic dipole operator Q_7. Examples of the corresponding contributions to the decay rate are shown in the subsequent columns of Fig. 5 as propagator diagrams with unitarity cuts. While G_{77} was found already several years ago [17], the complete calculation of G_{78} has been finalized only very recently [18]. Evaluation of G_{27} is still in progress (see below).

The remaining three cases (G_{22}, G_{28} and G_{88}) receive contributions from diagrams like those displayed in Fig. 6. Two-body final state contributions (first row) are just products of the known NLO amplitudes. Three- and four-body final state contributions remain unknown at the NNLO beyond the BLM approximation [19]. The BLM calculation for them has been completed very recently [20] providing new results for G_{88} and G_{28}, and confirming the old ones [21] for G_{22}. The overall NLO + (BLM-NNLO) contribution to the decay rate from three- and four-body final states in G_{22}, G_{28} and G_{88} remains below 4% due to the phase-space suppression by the relatively high photon energy cut E_0. Thus, the unknown non-BLM effects here can hardly cause uncertainties that could be comparable to higher-order $\mathcal{O}(\alpha_s^3)$ uncertainties in the dominant terms (G_{77} and G_{27}).

It follows that the only contribution that is numerically relevant but yet unknown at the NNLO is G_{27}. So far, it has been evaluated for arbitrary m_c in the BLM approximation [22, 21] supplemented by quark mass effects in loops on the gluon lines [23]. Non-BLM terms have been

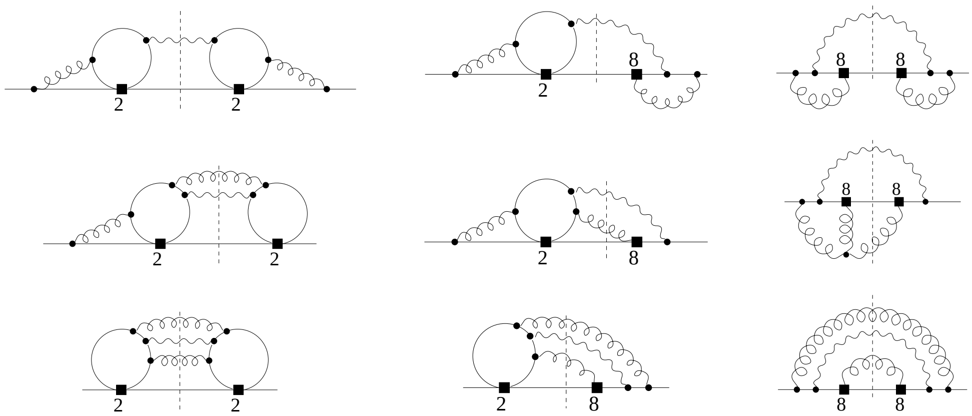

Figure 6: Examples of Feynman diagrams that contribute to G_{22}, G_{28} and G_{88} at $\mathscr{O}(\alpha_s^2)$.

calculated only in the $m_c \gg m_b/2$ limit [13, 24], and then interpolated downwards in m_c using BLM-based assumptions at $m_c = 0$. Such a procedure introduces a non-negligible additional uncertainty to the calculation, which has been estimated at the $\pm 3\%$ level in the decay rate.

As a first attempt to improve the situation, a calculation of G_{27} at $m_c = 0$ has been undertaken [25]. Two- and three-particle cut contributions have already been found [26]. A recently started calculation [27] for arbitrary m_c is supposed to cross-check the $m_c = 0$ result and, at the same time, make it redundant, because no interpolation in m_c will be necessary any more. The method to be used is the same as in the BLM calculation of Ref. [23].

As far as the non-perturbative effects are concerned, the question to what accuracy the approximate equality (5.3) holds has been subject of many investigations since early 1990's. However, a quantitative analysis of all the dominant contributions to the resulting uncertainty in $\mathscr{B}(\bar{B} \to X_s \gamma)$ has been performed only very recently [14]. Corrections to Eq. (5.3) are minimized at a certain "optimal" value of E_0 that is high enough ($E_0 \sim m_b/2$) but not too close to the endpoint ($m_b - 2E_0 \gg \Lambda$). The value of $E_0 = 1.6\,\text{GeV} \simeq m_b/3$ has a chance to be in the vicinity of the optimal point. In the following, I will discuss non-perturbative effects at this very cutoff, leaving aside the problem of photon energy extrapolation in the experimental averages.

So long as only the photonic dipole operator Q_7 is considered, non-perturbative corrections to Eq. (5.3) for $m_b - 2E_0 \gg \Lambda$ can be described in terms of the so-called fixed-order approach that has been derived [28] using the optical theorem and the Operator Product Expansion. The corrections can then be written as a series in $(\Lambda/m_b)^n \alpha_s^k$ with $n = 2, 3, 4, \ldots$ and $k = 0, 1, 2, \ldots$, where perturbatively calculable coefficients multiply matrix elements of local operators between the B-meson states at rest. Such matrix elements (at least the leading ones) can be extracted from measurements of observables that are insensitive to new physics, like the semileptonic $\bar{B} \to X_c e\nu$ decay spectra or mass differences between various b-flavored hadrons. Coefficients at the terms of order Λ^2/m_b^2 and Λ^3/m_b^3 have been evaluated in Refs. [29] and [30], respectively. Very recently, a calculation at order $\alpha_s \Lambda^2/m_b^2$ has been completed [31]. Thus, non-perturbative corrections to the "77" interference term are well under control.

The most important non-perturbative uncertainty originates from the "27" interference term (that stands for "27" and "17"). In Ref. [14], photons that can be treated in analogy to the "77" term

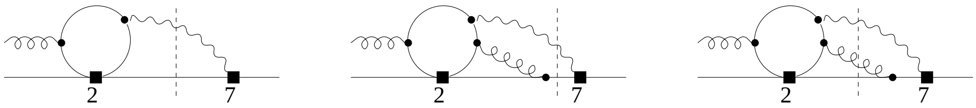

Figure 7: Examples of diagrams describing non-perturbative contributions to the "27" interference term due to soft gluons originating from the B-meson initial state.

are called "direct", while all the other ones are called "resolved", i.e. produced far away from the b-quark annihilation vertex. Contributions from the resolved photons can still be written in terms of a series in powers of $(\Lambda/m_b)^n \alpha_s^k$, but this time the $(n=1, k=0)$ term is non-vanishing when m_c is treated as $\mathscr{O}(\sqrt{\Lambda m_b})$. Moreover, they are uncertain, as they depend on matrix elements of non-local operators that cannot be easily extracted from other measurements. Diagrams representing such terms are displayed in Fig. 7, where the external gluon is understood to be soft, while the other one (if present) is considered to be non-soft.

If the charm quark was heavy enough ($m_c^2/m_b \gg \Lambda$), its loop in the first diagram of Fig. 7 would become effectively local for soft gluons, and we would be back to the local operator description, as in the "77" term. This limit has been analyzed in Refs. [32]. A series of the form

$$\sum_{n=0}^{\infty} b_n \mathscr{O}\left(\frac{\Lambda^2}{m_c^2} \left(\frac{m_b \Lambda}{m_c^2} \right)^n \right) \tag{5.5}$$

was found as a relative correction to Eq. (5.3). Explicit results for all the coefficients b_n showed that they are small and quickly decreasing with n, which led to a conclusion that the first term in the series is a good approximation to the whole correction even in the $m_b\Lambda/m_c^2 \sim \mathscr{O}(1)$ case. This conclusion has recently been questioned in Ref. [14] on the basis of realistic shape function models that allowed to vary m_c in the physically interesting range, and test applicability of the expansion (5.5). It has been found that the first term of such an expansion in not really a good approximation if we allow for alternating-sign subleading shape functions (see Eq. (108) in that paper). This is the main source of the overall $\pm 5\%$ non-perturbative uncertainty in the branching ratio that was estimated in Ref. [14]. So long as m_c is treated as $\mathscr{O}(\sqrt{\Lambda m_b})$, the considered correction is just $\mathscr{O}(\Lambda/m_b)$. Other (smaller) corrections studied in that paper were of order $\mathscr{O}(\alpha_s \Lambda/m_b)$.

In the end, let us recall that there exist non-perturbative corrections to Eq. (5.3) that are not suppressed by Λ/m_b at all. Their intuitive description can be found in Ref. [33]. In particular, collinear photon emission effects belong to this class [34, 20]. Fortunately, they are numerically small due to interplay of several minor suppression factors.

6. Summary

Measurements and calculations of radiative and rare semileptonic B decays have a long history but still offer realistic chances for improvements that could significantly strengthen constraints on the BSM theories. Many observables matter for models with sizeable new CP-violating phases or large deviations from the MFV hypothesis. In the MFV models with no new phases and $\mathscr{O}(1\,\text{TeV})$ masses, precision measurements of $B \to \mu^+\mu^-$ and $\bar{B} \to X_s \gamma$ are crucial. In the latter case, reduction of uncertainties by a factor of 2 on both the theoretical and experimental sides is feasible in the Super-B era.

References

[1] K. S. M. Lee, Z. Ligeti, I. W. Stewart and F. J. Tackmann, Phys. Rev. D **75** (2007) 034016 [hep-ph/0612156].

[2] T. Hurth and M. Nakao, arXiv:1005.1224.

[3] M. Beneke and T. Feldmann, Nucl. Phys. B **592** (2001) 3 [hep-ph/0008255].

[4] U. Egede, T. Hurth, J. Matias, M. Ramon and W. Reece, arXiv:1005.0571.

[5] M. Misiak, Nucl. Phys. B **393**, 23 (1993), Nucl. Phys. B **439**, 461 (1995) (E).

[6] A. Bharucha and W. Reece, Eur. Phys. J. C **69** (2010) 623 [arXiv:1002.4310].

[7] D. Asner *et al.* (Heavy Flavor Averaging Group), arXiv:1010.1589.

[8] M. Artuso, E. Barberio and S. Stone, PMC Phys. A **3** (2009) 3 [arXiv:0902.3743].

[9] S. Chen *et al.* (CLEO Collaboration), Phys. Rev. Lett. **87** (2001) 251807 [hep-ex/0108032].

[10] B. Aubert *et al.* (BABAR Collaboration), Phys. Rev. D **72** (2005) 052004 [hep-ex/0508004]; Phys. Rev. Lett. **97** (2006) 171803 [hep-ex/0607071]; Phys. Rev. D **77** (2008) 051103 [arXiv:0711.4889].

[11] K. Abe *et al.* (BELLE Collaboration), Phys. Lett. B **511** (2001) 151 [hep-ex/0103042]; A. Limosani *et al.* (Belle Collaboration), Phys. Rev. Lett. **103** (2009) 241801 [arXiv:0907.1384].

[12] M. Misiak *et al.*, Phys. Rev. Lett. **98** (2007) 022002 [hep-ph/0609232].

[13] M. Misiak and M. Steinhauser, Nucl. Phys. B **764** (2007) 62 [hep-ph/0609241].

[14] M. Benzke, S. J. Lee, M. Neubert and G. Paz, JHEP **1008** (2010) 099 [arXiv:1003.5012].

[15] C. Bobeth, M. Misiak and J. Urban, Nucl. Phys. B **574** (2000) 291 [hep-ph/9910220]; M. Misiak and M. Steinhauser, Nucl. Phys. B **683** (2004) 277 [hep-ph/0401041].

[16] M. Gorbahn and U. Haisch, Nucl. Phys. B **713** (2005) 291 [hep-ph/0411071]; M. Gorbahn, U. Haisch and M. Misiak, Phys. Rev. Lett. **95** (2005) 102004 [hep-ph/0504194]; M. Czakon, U. Haisch and M. Misiak, JHEP **0703** (2007) 008 [hep-ph/0612329].

[17] K. Melnikov and A. Mitov, Phys. Lett. B **620** (2005) 69 [hep-ph/0505097]; I. R. Blokland, A. Czarnecki, M. Misiak, M. Ślusarczyk and F. Tkachov, Phys. Rev. D **72** (2005) 033014 [hep-ph/0506055]; H. M. Asatrian, A. Hovhannisyan, V. Poghosyan, T. Ewerth, C. Greub and T. Hurth, Nucl. Phys. B **749** (2006) 325 [hep-ph/0605009]; H. M. Asatrian, T. Ewerth, A. Ferroglia, P. Gambino and C. Greub, Nucl. Phys. B **762** (2007) 212 [hep-ph/0607316]; H. M. Asatrian, T. Ewerth, H. Gabrielyan and C. Greub, Phys. Lett. B **647** (2007) 173 [hep-ph/0611123].

[18] H. M. Asatrian, T. Ewerth, A. Ferroglia, C. Greub and G. Ossola, arXiv:1005.5587; T. Ewerth, Phys. Lett. B **669** (2008) 167 [arXiv:0805.3911].

[19] S. J. Brodsky, G. P. Lepage and P. B. Mackenzie, Phys. Rev. D **28** (1983) 228.

[20] A. Ferroglia and U. Haisch, arXiv:1009.2144; M. Misiak and M. Poradziński, arXiv:1009.5685.

[21] Z. Ligeti, M.E. Luke, A.V. Manohar and M.B. Wise, Phys. Rev. D **60** (1999) 034019 [hep-ph/9903305].

[22] K. Bieri, C. Greub and M. Steinhauser, Phys. Rev. D **67** (2003) 114019 [hep-ph/0302051].

[23] R. Boughezal, M. Czakon and T. Schutzmeier, JHEP **0709** (2007) 072 [arXiv:0707.3090].

[24] M. Misiak and M. Steinhauser, Nucl. Phys. B **840** (2010) 271 [arXiv:1005.1173].

[25] R. Boughezal, M. Czakon and T. Schutzmeier, in preparation; M. Czakon, P. Fiedler, T. Huber and T. Schutzmeier, in progress.

[26] T. Schutzmeier, *Matrix elements for the $\bar{B} \to X_s \gamma$ decay at NNLO*, Ph.D. Thesis, University of Würzburg, 2009.

[27] M. Czakon, R. N. Lee, M. Misiak, A. V. Smirnov, V. A. Smirnov and M. Steinhauser, in progress.

[28] J. Chay, H. Georgi and B. Grinstein, Phys. Lett. B **247** (1990) 399.

[29] I.I. Bigi *et al.*, DPF92 Proceedings (Batavia, November 1992) [hep-ph/9212227]; A. F. Falk, M. E. Luke and M. J. Savage, Phys. Rev. D **49** (1994) 3367 [hep-ph/9308288].

[30] C. W. Bauer, Phys. Rev. D **57** (1998) 5611 [Erratum-ibid. D **60** (1999) 099907] [hep-ph/9710513].

[31] T. Ewerth, P. Gambino and S. Nandi, Nucl. Phys. B **830** (2010) 278 [arXiv:0911.2175].

[32] G. Buchalla, G. Isidori and S.J. Rey, Nucl. Phys. B **511** (1998) 594 [hep-ph/9705253]; Z. Ligeti, L. Randall and M.B. Wise, Phys. Lett. B **402** (1997) 178 [hep-ph/9702322]; A.K. Grant, A.G. Morgan, S. Nussinov and R.D. Peccei, Phys. Rev. D **56** (1997) 3151 [hep-ph/9702380]; M.B. Voloshin, Phys. Lett. B **397** (1997) 275 [hep-ph/9612483]; A. Khodjamirian, R. Rückl, G. Stoll and D. Wyler, Phys. Lett. B **402** (1997) 167 [hep-ph/9702318].

[33] M. Misiak, Acta Phys. Polon. B **40** (2009) 2987 [arXiv:0911.1651].

[34] A. Kapustin, Z. Ligeti and H.D. Politzer, Phys. Lett. B **357** (1995) 653 [hep-ph/9507248].